Gadolinium: A helical antiferromagnet or a collinear ferromagnet

S. N. Kaul* and S. Srinath
School of Physics, University of Hyderabad, Central University P.O., Hyderabad 500 046, Andhra Pradesh, India
(Received 17 November 1999)

Contrary to the recent claim that gadolinium behaves as an antiferromagnet with a helical spin structure for temperatures between the spin reorientation (SR) temperature T_{SR} and the Néel point, the ac susceptibility and low-field bulk magnetization data taken along the [0001] and [$10\bar{1}0$] hexagonal directions of high-purity gadolinium single crystals over a wide range of temperatures provide ample experimental evidence in favor of the widely accepted view that gadolinium is a normal ferromagnet with a *collinear* spin structure in the temperature range from T_{SR} to the Curie point T_C. However, the magnetic behavior of gadolinium is complicated by a rather complex temperature dependence of the easy direction of magnetization for temperatures below T_{SR}.

I. INTRODUCTION

Nearly four decades ago, Belov and Pedko[1] observed anomalies in thermomagnetic curves and kinks in magnetization isotherms of *polycrystalline* gadolinium (Gd) at low fields ($H_{ext} \leqslant 15$ Oe), and temperatures ranging between $T_1 = 210$ K and the Curie point $T_C \simeq 293$ K. Since these kinks are reminiscent of those reported previously in dysprosium at the critical fields that mark the disappearance of ''helical'' antiferromagnetism, Belov and Pedko[1] concluded that a *helical* spin structure similar to that prevalent in the other heavy rare-earth metals also exists in Gd in the temperature range $T_1 \leqslant T \leqslant T_C$, with the only difference that external magnetic fields (H_{ext}) as low as 15 Oe suffice to transform the helical spin structure (a special type of antiferromagnetic order) into a collinear one (ferromagnetic order) in Gd. Such a notion about the spin structure in Gd had to be discarded after subsequent magnetic investigations[2–5] on Gd *single crystals* failed to reproduce such anomalies or kinks in low-field magnetization, and neutron-diffraction measurements[6,7] did not reveal any satellite reflections characteristic of helical spin structures. Consistent with the temperature variations of the magnetocrystalline anisotropy constants[8,9] K_1 and K_2, neutron-diffraction data[6,7] demonstrated that Gd is a normal ferromagnet with a rather complex[6–10] temperature dependence of the spontaneous moment alignment. The direction of magnetic moments is *parallel* to the hexagonal *c* axis from T_C down to the spin-reorientation (SR) temperature T_{SR} of 230 K (where K_1 changes[8,9] sign and K_2 is vanishingly small[8,9]), moves away from the *c* axis for $T < T_{SR}$ to a maximum tilt angle of about 60° near $T^* = 180$ K, and then tilts back to within 30° of the *c* axis at low temperatures. The view that Gd is a simple ferromagnet has gained wide acceptance over the years.

Based on the observation that the initial susceptibility $\chi_{ext}(T) = M(T)/H_{ext}$ of the needle-shaped single crystals of gadolinium is not *demagnetization limited* at T_C but at T_{SR}, it has recently been claimed[11] that the magnetic order in Gd for temperatures between T_{SR} and T_C is not truly ferromagnetic, but is akin to the helical spin structure previously found in erbium. In this paper, we report the $\chi_{ext}(T)$ data taken along different crystallographic directions on high-purity Gd single crystals five years ago, when we embarked upon a detailed study of critical-point phenomena in Gd. These hitherto unpublished data not only reproduce the observations made recently by Coey *et al.*[11] and reveal their exact origin, but also assert that Gd, far from being an antiferromagnet with helical spin structure, is a simple ferromagnet with collinear spin configuration for temperatures in the vicinity of T_C.

II. EXPERIMENTAL DETAILS

Two types of high-purity (99.92 at. %) single crystals,[12] one of them grown without making any attempt to correct the misalignment between the *c* axis and the cylindrical/rod axis (the so-called ''as-grown'' crystal), and the other spark-machined such that the cylindrical axis coincided with the *c* axis to within[12] 0.1° before subjecting the rod (1.8 mm in diameter) to the solid state electrotransport treatment (henceforth referred to as the ''oriented'' crystal), have been used in this work. Since the as-grown crystal rod was not uniform in diameter, it was spark-machined to a diameter of 1.55 mm, and a portion of 26.8-mm length (sample 1) was spark-cut. Two cylindrical samples of dimensions 1.5 (diameter) × 1.7 (length) mm (sample 2) and 1.60×1.83 mm^2 (sample 3) were spark-cut from the oriented crystal rod.[12] X-ray Laue patterns of various portions along the length of sample 1 revealed that the *c* axis lies on a cone around the cylindrical axis and the cone angle varies *erratically* from 2° to about 10° along the length mainly due to twinning. It is well known[13,14] that twinning invariably occurs in large single crystals of Gd with a low oxygen content.

Real [$\chi'_{ext}(T)$] and imaginary [$\chi''_{ext}(T)$] components of susceptibility at different but fixed (to within ±5 mK) temperatures were measured[12] on thin cylindrical samples 1 and 2 in the presence or absence of a superposed dc magnetic field (H_{dc}) at various fixed frequencies (18.7 Hz $\leqslant \nu \leqslant$ 870 Hz) and rms amplitudes (1 mOe $\leqslant H_{ac} \leqslant$ 1 Oe) of an ac driving field (H_{ac}), with H_{ac} and/or H_{dc} directed along some crystallographic direction or cylindrical axis. When $H_{dc} = 0$ and $H_{ac} \neq 0$, $\chi'_{ext}(T)$ and $\chi''_{ext}(T)$ measurements were performed after compensating for the Earth's magnetic field. Magnetization M was measured as a function of H_{ext} ($\equiv H_{dc}$) in the field range -100 Oe $\leqslant H_{ext} \leqslant 100$ Oe at fixed temperatures ranging between 100 and 300 K on samples 2

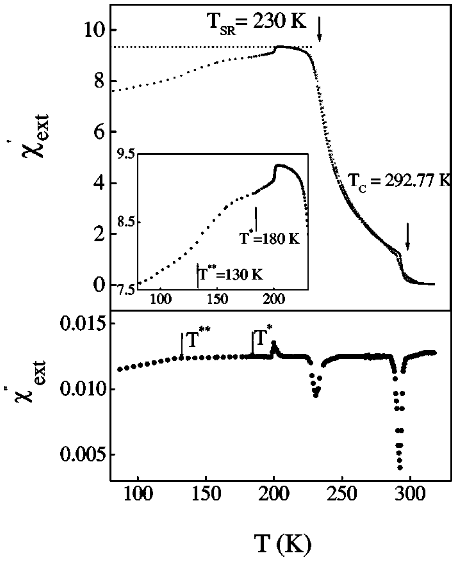

FIG. 1. Temperature dependence of the real, χ'_{ext}, and imaginary, χ''_{ext}, components of the susceptibility, when an ac field of amplitude H_{ac} and frequency 87 Hz is applied along the cylindrical axis of sample 1 ($H_{ac}=10$ m Oe, closed circles; $H_{ac}=1$ Oe, crosses). The inset shows the enlarged view of the $\chi'_{ext}(T)$ data in the temperature range from 80 to 230 K. The horizontal dashed line indicates the demagnetization-limited value $\chi'_{ext}=1/4\pi N_d$.

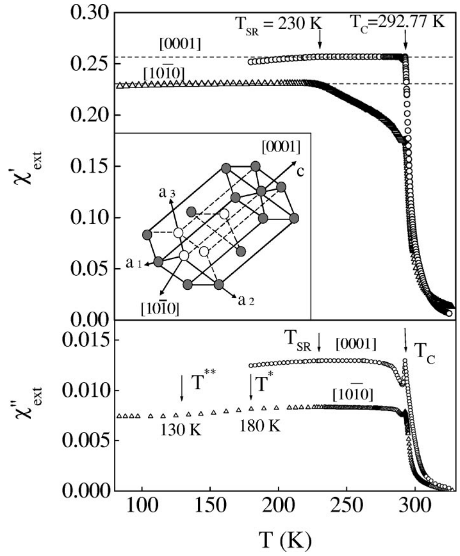

FIG. 2. Temperature dependence of the real, χ'_{ext}, and imaginary, χ''_{ext}, components of the susceptibility for sample 2, when an ac field of amplitude H_{ac} = 10 m Oe and a frequency of 87 Hz is applied in the [0001] (open circles) and [10$\bar{1}$0] (open triangles) crystallographic directions. The inset displays the hexagonal close-packed structure of gadolinium, and indicates the crystallographic directions along which $\chi'_{ext}(T)$ and $\chi''_{ext}(T)$ were measured on sample 2. Horizontal dashed lines indicate the demagnetization-limited values ($=1/4\pi N_d$).

and 3 when H_{ext} was directed along the c axis (same as the cylindrical axis).

III. RESULTS AND DISCUSSION

Figures 1 and 2 display $\chi'_{ext}(T)$ and $\chi''_{ext}(T)$ data obtained when $H_{dc}=0$ and H_{ac} ($\equiv H_{ext}$) of rms amplitude 10 m Oe and frequency 87 Hz is applied along the cylindrical axis in sample 1 (closed circles, Fig. 1) and along the directions *parallel* (c axis or the [0001] direction (inset of Fig. 2), open circles) and *perpendicular* (the [10$\bar{1}$0] direction in the basal plane (inset of Fig. 2), open triangles) to the cylindrical axis in sample 2 (Fig. 2). Besides presenting an enlarged view of the $\chi'_{ext}(T)$ data taken at $H_{ac}=10$ m Oe and $\nu=87$ Hz in the temperature range 80 K $\leqslant T \leqslant$ 230 K on sample 1 in the inset, Fig. 1 depicts the temperature variation of χ'_{ext} for sample 1 when $H_{ac}=1$ Oe at $\nu=87$ Hz is applied along the cylindrical axis (crosses). The hexagonal close-packed structure of Gd as well as the crystallographic directions along which H_{ac} has been applied in sample 2 are depicted in the inset of Fig. 2. The enlarged view serves to highlight the structure observed in the $\chi'_{ext}(T)$ curve at temperatures $T^*=180$ K and $T^{**}=130$ K, in addition to that noticed at $T_{SR}=230$ K and $T_C=292.77$ K in this curve in the main figure. The corresponding structure at these temperatures is apparent in the $\chi'_{ext}(T)$ and $\chi''_{ext}(T)$ curves for sample 2 (Fig. 2) as well.

One of the characteristic properties of ferromagnets is the *divergence* of *intrinsic* magnetic susceptibility χ_{int} along the *easy* direction of magnetization (i.e., the magnetization direction *favored* by magnetocrystalline anisotropy in the absence of H_{ext}) at T_C. When both shape as well as magnetocrystalline anisotropies are present, $\chi_{int}(T)$ is related to the measured initial susceptibility $\chi_{ext}(T)$ as

$$\chi_{int}^{-1}(T)=\chi'^{-1}_{ext}(T)-4\pi N(T), \tag{1}$$

where[15] $N(T)=N_d+N_K(T)$, the demagnetization factor N_d depends only on the sample shape, $H_d=4\pi N_d M$ is the demagnetizing field, and the quantity $N_K(T)$, in its most general form for a spin system with hexagonal crystal structure and exhibiting (uniaxial) magnetocrystalline anisotropy, is given by[16]

$$N_K(T)=H_K(T)/4\pi M_S(T)=[2\cos\theta(T)/4\pi M_S^2(T)][K_1(T)+2K_2(T)\sin^2\theta(T)]. \tag{2}$$

In Eq. (2), H_K is the *uniaxial* anisotropy field, M_S is the spontaneous magnetization, and θ is the angle that M_S makes with the c axis or the [0001] direction in the crystal with hexagonal structure (inset of Fig. 2). Note that Eq. (2) is valid for *finite* θ but not for $\theta=0^0$ when $N_K=0$. According to Eq. (1), χ_{int} diverges at a temperature T_0 where $\chi'_{ext}(T_0)=1/4\pi N(T_0)$; T_0 can be significantly different from T_C if $N_K(T_C)\neq 0$. Alternatively, the uniaxial magnetocrystalline anisotropy introduces a temperature scale of its own, and causes a *shift*[17] in the Curie temperature of an otherwise isotropic ferromagnet.

In order to understand the temperature variations of χ'_{ext} in different crystallographic directions, three cases need to be distinguished. *Case I*: H_{ext} is applied along the *easy* direction of magnetization (e.g., the [0001] direction in Gd for temperatures between T_{SR} and T_C), for which the magnetocrystalline anisotropy energy E_K is *minimum*, and as a result[15] N_K = 0 (since H_{ext} does not have to do any work against H_K and the presence of H_K is not felt at all). As a consequence, χ'_{ext} gets *limited* at the value of $1/4\pi N = 1/4\pi N_d$ (the demagnetization-limited value) from T_C (where $\chi_{int}^{-1}=0$) down to T_{SR}. *Case II*: H_{ext} points in the *hard* direction (e.g., the $[10\bar{1}0]$ direction in Gd), for which E_K is *maximum* and $4\pi N_K = 2K_1/M_S^2$ is sizable since K_1 is large. χ'_{ext} $(=1/4\pi N)$ attains a value at T_C which lies well below the demagnetization limit since $N_K > N_d$, increases with decreasing temperature because K_1 (and hence N_K) decreases,[8,9] and reaches the demagnetization limit at T_{SR} where[8,9] $K_1=0$ (consequently, $N_K=0$); note that $K_2=0$ in the range $T_{SR} \leqslant T \leqslant T_C$. *Case III*: H_{ext} is applied along the sample dimension for which N_d has the smallest value (e.g., the cylindrical axis of sample 1), but this direction is neither parallel nor perpendicular to the direction favored by magnetocrystalline anisotropy, i.e., the case when $N_d \leqslant N_K$. With decreasing temperature, χ'_{ext} rises steeply from a small value $\approx 1/4\pi N_K$ at T_C (since N_K is large) to a large value $= 1/4\pi N_d$ at T_{SR} (since $N_K=0$, and N_d is extremely small).

The results presented in Figs. 1 and 2, when viewed in the light of above remarks, assert that the variations of χ'_{ext} with temperature for sample 2 when H_{ac} is applied (i) along the c axis $[N_d=0.31(1)]$ (open circles) and (ii) perpendicular to the c axis (i.e., along the $[10\bar{1}0]$ direction) $(N_d=0.345)$ (open triangles), respectively, are the experimental realizations of cases I and II, while $\chi'_{ext}(T)$ for sample 1 $(N_d = 0.0085)$ (closed circles) corresponds to case III. Note that the horizontal dashed lines indicate the demagnetization-limited values $(=1/4\pi N_d)$ for the sample-H_{ac} configurations in question. Common to all three cases is the decline in $\chi'_{ext}(T)$ for $T<T_{SR}$ (Figs. 1 and 2) from the demagnetization-limited value at $T=T_{SR}$ where shape anisotropy favors the cylindrical axis as the easy direction of magnetization. χ'_{ext} decreases as the temperature is lowered below T_{SR}, because a change in the direction of H_K (or equivalently, in the easy direction of magnetization) at such temperatures takes the magnetization vector *away* from the H_{ext} direction. The structure observed in $\chi'_{ext}(T)$ curves at T^* and T^{**} is, therefore, a manifestation of the peak at $T^* \simeq 180$ K and the crossover from rapid to slow variation at $T^{**} \simeq 130$ K in the $\theta(T)$ curve.[6–10] As expected, the features observed in the $\chi'_{ext}(T)$ curves at T_C, T_{SR}, T^*, and T^{**} are apparent in the $\chi''_{ext}(T)$ curves (Figs. 1 and 2) as well. In addition to these common features, $\chi'_{ext}(T)$ $[\chi''_{ext}(T)]$ exhibits an abrupt drop (a small *peak*) at $T^{\dagger} \simeq 200$ K in sample 1. This feature, unique to sample 1, finds the following explanation. While the sample is cooled below T_{SR}, magnetocrystalline anisotropy continuously grows in strength such that when the temperature $T^{\dagger}$ is reached, even the relatively large shape anisotropy in this sample can no longer hold the magnetizations of twinned crystals (that constitute sample 1) parallel to the cylindrical axis (or $\mathbf{H}_{ext}$) against the tendency of magnetocrystalline anisotropy to ''unfurl'' these magnetizations into cones with the cone angle varying along the length. A sudden unfurling of the magnetizations away from the direction of H_{ext} at $T^{\dagger}$ results in an abrupt drop in χ'_{ext}, and the variation of χ'_{ext} with temperature for $T<T^{\dagger}$ is essentially dictated by magnetocrystalline anisotropy. Another aspect in which sample 1 distinguishes itself from the other two samples is that as low a field as $H_{ac}=1$ Oe suffices to smear the transition at T_C (Fig. 1). The sensitivity of the transition to H_{ac} in this particular case can be understood as follows. Contrasted with a unique value for N_K at a given temperature yielded by Eq. (2) for samples 2 and 3, the N_K values for sample 1 at any temperature are *distributed* around some average value due to the variation in the tilt angle between the c axis and the cylindrical axis along the sample length even for temperatures in the range $T_{SR} \leqslant T \leqslant T_C$. A distribution in the N_K values leads to a marked nonlinearity in the $M-H_{ext}$ isotherms even at extremely low fields. Consequently, an increase in the value of H_{ac} from 10 m Oe to 1 Oe slows down the temperature variation of χ'_{ext} for temperatures in the vicinity of T_C.

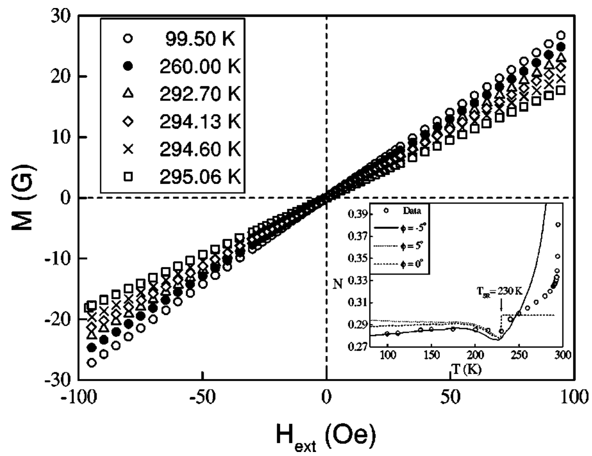

FIG. 3. Magnetization as a function of the external magnetic field in the range -100 Oe$\leqslant H_{ext} \leqslant 100$ Oe at a few selected values of temperature. The inset shows the temperature dependence of the quantity N (open circles) and the theoretical variations (curves) explained in the text.

Figure 3 displays the low-field $(-100$ Oe $\leqslant H_{ext} \leqslant 100$ Oe) portions of a few representative $M-H_{ext}$ isotherms taken on sample 3 in the temperature range 100 K$\lesssim T \lesssim 300$ K when H_{ext} is applied along the cylindrical axis (which is also the c axis in this case). According to Eq. (1), the *inverse* slope of each straight line $M-H_{ext}$ isotherm equals the $4\pi N$ value at that temperature if $\chi_{int}(T)$ is extremely large. The values of N at different temperatures, so determined, are plotted against temperature (open circles) in the inset of Fig. 3, and compared with the corresponding theoretical estimates for three different cases: (i) $\phi=0$ (dashed curve), (ii) $\phi=-5°$ (continuous curve) and (iii) $\phi = 5°$ (dotted curve), arrived at as follows. The theoretical values of $N_K(T)$, computed from Eq. (2) using the reported values[7–10,18] of $K_1(T), K_2(T), \theta(T)$, and $M_S(T)$, and that of N_d, calculated using the relation $N_d = N_c \cos\phi + (1/2)(1 - N_c)\sin\phi$ (where ϕ is the angle between H_{ext} and c axis, and $N_c = N_d = 0.298$ is the demagnetizing factor when $\phi = 0°$), are inserted into the relation $N(T) = N_d + N_k(T)$ to obtain $N(T)$. As far as the calculation of $N_K(T)$ is concerned, these cases represent the situations where there is a constant shift of $0°$, $-5°$, and $5°$ in the reported values of $\theta(T)$, i.e., $\theta(T)$ in Eq. (2) is replaced by $\theta(T)+\phi$. Such a comparison reveals that the experimental data are best described by the theoretical curve for which $\phi = -5°$. The discrepancy between theory and experiment observed at $T \gtrsim T_{SR}$ is not serious, since the values of K_1 and K_2 at T

$\approx T_{SR}$, being vanishingly small, have large uncertainties, and the ''forced'' magnetization contribution at finite fields (which is particularly important for $T \approx T_C$) has not been taken into account in the calculation of $N_K(T)$. Note that the theoretical curves for $\phi = \pm 5°$ exhibit a steep rise as $T \rightarrow T_C$, because $M_S \rightarrow 0$ [consequently, N_K in Eq. (2) blows up] in this limit and that T_C (possesses the same value for samples 2 and 3) has been accurately determined by several independent methods described in detail in Refs. 12 and 18. A similar set of $N(T)$ data taken on[18] sample 2 showed a *much weaker* (by nearly a factor of 3) dependence of N on T for $T \gtrsim T_{SR}$, and Eq. (2) with $\phi = 2°$ provides a very good fit to the $N(T)$ data. In magnetization measurements that involve sample movement and sample mounting on long holder rods, such a residual misalignment between the field direction and the c axis or cylindrical axis is inevitable. Since the method used by us to measure ac susceptibility does not require sample transport and long sample-holder rods, the cylindrical axis and/or the crystallographic directions [0001] and $[10\bar{1}0]$ could be aligned with the field direction to an accuracy better than $\pm 0.5°$ with ease. From the $N(T)$ data displayed in the inset of Fig. 3, it is clear that the value of N_K (and hence of N) rises sharply as $T \rightarrow T_C$, even when there is a slight misalignment between the direction of H_{ext} and the cylindrical axis or the [0001] direction. Consequently, χ'_{ext} is limited to a much lower value at T_C than the demagnetization-limited value of $1/4\pi N_d$. However, $N = N_d$ for temperatures in the range $T_{SR} \leqslant T \leqslant T_C$, when the direction of H_{ext} exactly coincides with the [0001] direction (the $\phi = 0^0$ case in Fig. 3). Only in this case, $\chi'_{ext}(T)$ is demagnetization limited at T_C, and the intrinsic susceptibility diverges at T_C.

IV. CONCLUSION

A detailed discussion of the ac susceptibility and low-field bulk magnetization data taken along different crystallographic directions and/or the cylindrical axis of several high-purity gadolinium single crystals over a wide temperature range reveals that Gd is a normal ferromagnet, with the only complication that the easy direction of magnetization changes with temperature in a rather complex manner for temperatures below the spin-reorientation temperature T_{SR}. Our results thus refute the recent claim[11] that Gd behaves as an antiferromagnet with a helical spin structure for temperatures between T_{SR} and the Néel point ($\equiv T_C$).

A striking resemblance between the $\chi'_{ext}(T)$ curves obtained by us for sample 1 and by Coey *et al.*[11] for a needle-shaped sample with H_{ac} parallel to the c axis $[\chi'_{\parallel}(T)]$ permits us to conclude that in the needle-shaped sample of Coey *et al.*, as in our sample 1, the c axis lies on a cone around the long axis of the crystal, and the cone angle varies along the length due to twinning and other faults developed during crystal growth. Since the c axis is the easy direction of magnetization for temperatures ranging between T_{SR} and T_C, a variation in the c-axis direction simulates a helical-like spin structure which, in turn, prevents the intrinsic susceptibility from diverging at T_C. However, this is not an intrinsic property of Gd but an artifact of the growth process. Our results on high-purity Gd single crystals (sample 2) clearly demonstrate that the c-axis *intrinsic* susceptibility *diverges* (Fig. 2) at T_C, as is expected[12,18] for a ferromagnet with uniaxial anisotropy.

The results presented in the inset of Fig. 3 provide yet another possible explanation for the $\chi'_{\parallel}(T)$ data reported recently by Coey *et al.*[11] A situation similar to case III, described in Sec. III, arises even for a perfect (twinning-free) Gd single crystal if the direction of H_{ext} does not exactly coincide with the c axis. In view of the general (and our own) experience in the growth of long Gd single crystals with a low oxygen content, we consider the first explanation as the more likely one

---

*Author to whom correspondence should be addressed. Email address: kaulsp@uohyd.ernet.in

[1] K. P. Belov and A. V. Ped'ko, Zh. Éksp. Teor. Fiz. **47**, 87 (1962) [Sov. Phys. JETP **15**, 62 (1962)].

[2] H. E. Nigh, S. Legvold, and F. H. Spedding, Phys. Rev. **132**, 1092 (1963).

[3] C. D. Graham, Jr., Jpn. J. Appl. Phys. **36**, 1135 (1965).

[4] Kh. K. Aliev, I. K. Kamilov, and A. M. Omarov, Zh. Éksp. Teor. Fiz. **94**, 153 (1988) [Sov. Phys. JETP **67**, 2262 (1988)].

[5] S. Yu. Dan'kov, A. M. Tishin, V. K. Pecharsky, and K. A. Gschnidner, Jr., Phys. Rev. B **57**, 3478 (1998).

[6] G. Will, R. Nathans, and H. A. Alperin, J. Appl. Phys. **35**, 1045 (1964).

[7] J. W. Cable and E. O. Wollan, Phys. Rev. **165**, 733 (1968).

[8] W. D. Corner, W. C. Roe, and K. N. R. Taylor, Proc. Phys. Soc. London **80**, 927 (1962).

[9] C. D. Graham, Jr., J. Phys. Soc. Jpn. **17**, 1310 (1962); J. Appl. Phys. **34**, 1341 (1963).

[10] W. D. Corner and B. K. Tanner, J. Phys. C **9**, 627 (1976).

[11] J. M. D. Coey, V. Skumryev, and K. Gallagher, Nature (London) **401**, 35 (1999).

[12] S. Srinath, S. N. Kaul, and H. Kronmüller, Phys. Rev. B **59**, 1145 (1999).

[13] J. J. Brissot and R. Martres, J. Appl. Phys. **36**, 3360 (1965); M. Whittaker, J. Cryst. Growth **3**, 317 (1968).

[14] B. J. Beaundry and K. A. Gschneidner, Jr., in *Handbook on the Physics and Chemistry of Rare Earths*, edited by K. A. Gschneidner, Jr. and L. Eyring (North-Holland, Amsterdam, 1978), p. 173.

[15] C. Kittel, Phys. Rev. **73**, 155 (1948); S. N. Kaul and V. Siruguri, J. Phys.: Condens. Matter **4**, 505 (1992).

[16] F. Brailsford, *Physical Principles of Magnetism* (Van Nostrand, London, 1966), pp. 124–128, 193, and 194.

[17] D. J. W. Geldart, P. Hargraves, N. M. Fujiki, and R. A. Dunlap, Phys. Rev. Lett. **62**, 2728 (1989); R. A. Dunlap, N. M. Fujiki, P. Hargraves, and D. J. W. Geldart, J. Appl. Phys. **76**, 6338 (1994); E. R. Callen, Phys. Rev. **124**, 1373 (1961).

[18] S. Srinath and S. N. Kaul, Phys. Rev. B **60**, 12 166 (1999).